JACS
JOURNAL OF THE AMERICAN CHEMICAL SOCIETY
Article
pubs.acs.org/JACS

Direct Detection of a Triplet Vinylnitrene, 1,4-Naphthoquinone-2-ylnitrene, in Solution and Cryogenic Matrices

Sujan K. Sarkar,[†] Asako Sawai,[‡] Kousei Kanahara,[‡] Curt Wentrup,[§] Manabu Abe,[‡] and Anna D. Gudmundsdottir*[,†]

[†]Department of Chemistry, University of Cincinnati, Cincinnati, Ohio 45221-0172, United States

[‡]Department of Chemistry, Graduate School of Science, Hiroshima University, 1-3-1 Kagamiyama, Higashi-Hiroshima, Hiroshima 739-8526, Japan

[§]School of Chemistry and Molecular Biosciences, The University of Queensland, Brisbane, Queensland 4072, Australia

Supporting Information

ABSTRACT: The photolysis of 2-azido-1,4-naphthoquinone (**1**) in argon matrices at 8 K results in the corresponding triplet vinylnitrene ^{3}**2**, which was detected directly by IR spectroscopy. Vinylnitrene ^{3}**2** is stable in argon matrices but forms 2-cyanoindane-1,3-dione (**3**) upon further irradiation. Similarly, the irradiation of azide **1** in 2-methyltetrahydrofuran (MTHF) matrices at 5 K resulted in the ESR spectrum of vinylnitrene ^{3}**2**, which is stable up to at least 100 K. The zero-field splitting parameters for nitrene ^{3}**2**, D/hc = 0.7292 cm^{-1} and E/hc = 0.0048 cm^{-1}, verify that it has significant 1,3-biradical character. Vinylnitrene ^{3}**2** (λ_{max} ~ 460 nm, τ = 22 μs) is also observed directly in solution at ambient temperature with laser flash photolysis of **1**. Density functional theory (DFT) calculations support the characterization of vinylnitrene ^{3}**2** and the proposed mechanism for its formation. Because vinylnitrene ^{3}**2** is relatively stable, it has potential use as a building-block for high-spin assemblies.

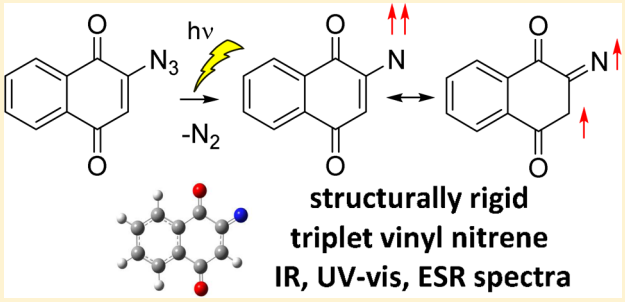

INTRODUCTION

Nitrenes are electron-deficient reactive intermediates that have two unpaired electrons and can thus have triplet or singlet configurations.[1,2] Singlet nitrenes are mostly short-lived and decay by intramolecular reactivity. However, some singlet nitrenes are sufficiently long-lived to undergo bimolecular reactions and have therefore been used in various applications, such as the cross-linking of polymers,[3] surface alteration,[4] and photoaffinity labeling.[5] In comparison, the high-spin properties of triplet nitrenes make them potential building units for high-spin assemblies.[6] Because of the various applications of nitrenes, there is a general interest in them.

We have reported the first detection of triplet vinylnitrenes in solution by performing laser flash photolysis of azirine and isoxazole derivatives (Scheme 1).[7−9] The vinylnitrenes were formed by using built-in triplet sensitizers, which made it possible to form the triplet vinylnitrenes without having to depend on intersystem crossing from singlet to triplet vinylnitrenes. However, the photolysis of these azirines in cryogenic matrices yielded ketenimine derivatives (Scheme 2), not vinylnitrenes, although the ketenimines are likely to be formed from vinylnitrene intermediates. Similarly, Inui et al. have shown that the irradiation of naphthyl azirines in cryogenic matrices yields ketenimine products. Nunes et al. reported that the photolysis of isoxazole derivatives in cryogenic matrices can be used to convert them to the corresponding azirines, presumably through triplet vinylnitrenes.[10−13] However, no reported studies have verified that these conversions take place through triplet vinylnitrene intermediates, as vinylnitrenes have not been directly detected in cryogenic matrices. Thus, the question arises why simple triplet vinylnitrenes are not stable in cryogenic matrices, unlike other triplet nitrenes, such as alkyl- and phenylnitrenes. Triplet alkyl- and arylnitrenes are generally long-lived intermediates

Scheme 1. Photochemistry of Azirine and Isoxazole Derivatives

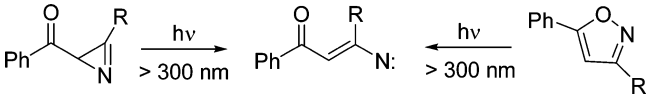

Scheme 2. Formation of Ketenimines in Argon Matrices

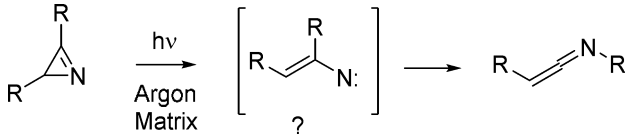

Received: January 29, 2015
Published: March 11, 2015

DOI: 10.1021/jacs.5b00998
J. Am. Chem. Soc. 2015, 137, 4207−4214

that decay by dimerization rather than intersystem crossing or reacting with the solvent and have been characterized directly in both solution and cryogenic matrices.[14,15] Intriguingly, Wentrup and Kvaskoff reported that highly conjugated triplet dienylnitrenes are stable in cryogenic matrixes.[16]

Recently, we established that the triplet sensitization of a vinyl azide can be used to form a vinylnitrene intermediate.[17] As vinyl azides are more versatile precursors than azirine or isoxazole derivatives, they enable the formation of a wide variety of vinylnitrenes with different and complex structures.

In this Article, we studied the vinylnitrene formed from the bicyclic 2-azido-1,4-naphthoquinone **1** (Scheme 3). By

Scheme 3. Proposed Mechanism for Forming Triplet Vinylnitrene ^{3}2 and Nitrile 3 from 1

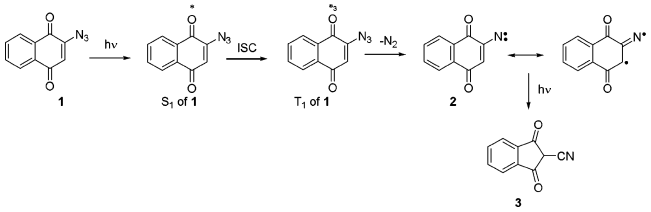

irradiating the rigid vinyl azide **1** with a built-in triplet sensitizer, it becomes possible to form triplet vinylnitrene ^{3}**2**, which can be detected directly in cryogenic matrices using IR and ESR (electron spin resonance) spectroscopy, as it is stable up to at least 100 K. Under the irradiation conditions, the triplet nitrene ^{3}**2** was found to rearrange to a nitrile **3**.

RESULTS

Matrix IR Spectroscopy. Vinyl azide **1** was deposited into an argon matrix at 8 K by heating it to 50 °C while using argon to entrain the vapor. The matrix was irradiated with a xenon lamp through a 320−360 nm filter for 20.5 min. The characteristic IR bands of the azide chromophore at 2129, 2118, and 2107 cm^{-1} were almost fully depleted after 2 min of irradiation (Figure 1), along with bands at 1683, 1664, 1661,

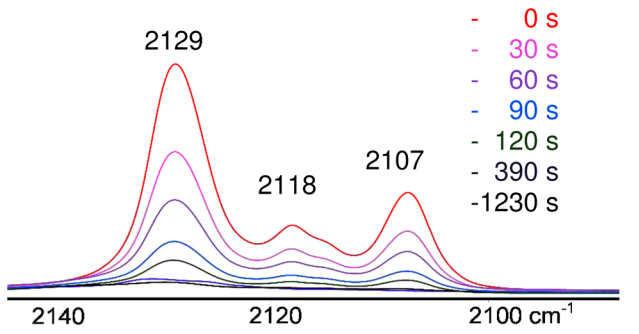

Figure 1. Depletion of the azide bands of azide **1** upon irradiation in argon matrices at 8 K.

1605, 1600, 1578, 1372, 1324, 1273, 944, 885, 741, 716, 644, and 594 cm^{-1} (Figure 2A). Concurrently with the depletion of these bands, two sets of new bands were formed. The intensities of the bands that formed at 1705, 1345, 1325, 1270, 962, and 701 cm^{-1} increased with irradiation time for the first 120 s and then decreased with further irradiation until they were almost fully depleted after 20.5 min of irradiation. These bands are assigned to the triplet vinylnitrene ^{3}**2** on the basis of

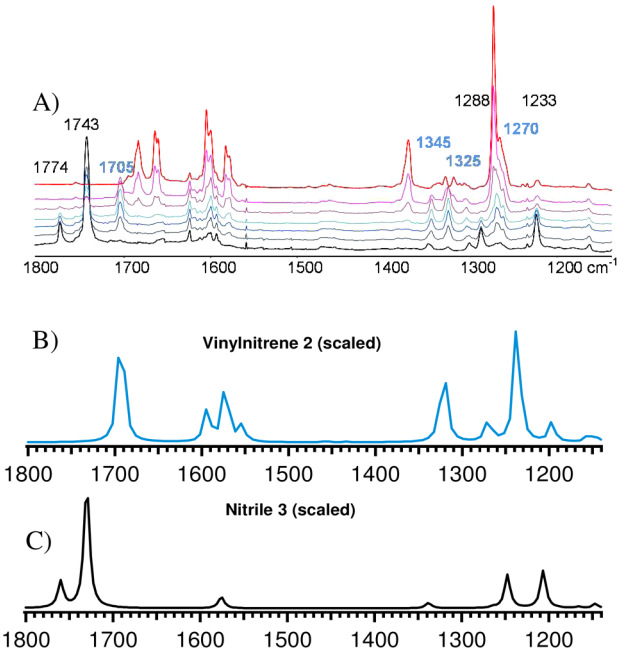

Figure 2. (A) IR spectra obtained before (red) and after (blue to black) irradiating **1** in argon matrix at 8 K. Calculated IR spectrum at the B3LYP/6-31+G(d) level for (B) vinylnitrene ^{3}**2** and (C) nitrile **3** after scaling by 0.9613.[18] The difference IR spectra after 60 and 1230 s are displayed in Supporting Information Figure S1.

comparisons with the calculated spectrum (Figure 2B). The most intensive band at 1705 cm^{-1} is assigned to the C═O stretch of the carbonyl group next to the nitrene center, which is calculated to be located at 1761 cm^{-1}, and scaling by 0.9613[18] places it at 1693 cm^{-1}. We assign the band at 1345 cm^{-1} to the C−N stretch in vinylnitrene ^{3}**2**, which is calculated to be located at 1375 cm^{-1}, and scaling places it at 1322 cm^{-1}. The band at 1325 cm^{-1} is assigned to the coupled C−C stretches calculated at 1321 cm^{-1}, which scaling places at 1270 cm^{-1}. A set of bands formed at 1774, 1743, 1288, 1233, 1135, 938, 930, 825, and 682 cm^{-1} as the bands due to vinylnitrene ^{3}**2** were depleted, and these bands are assigned to nitrile **3** on the basis of comparison with its calculated spectrum (Figure 2C). The bands at 1774 and 1743 cm^{-1} are assigned to the symmetrical and antisymmetrical stretches of C═O bands, which are calculated at 1831 and 1800 cm^{-1}, respectively, and 1760 and 1730 cm^{-1}, respectively, with scaling. Furthermore, we assign the bands at 1288 and 1233 cm^{-1} to C−C stretching, calculated to be at 1298 and 1255 cm^{-1}, and scaled to be at 1248 and 1206 cm^{-1}, respectively. The CN stretching in nitrile **3** is located at 2271 cm^{-1} as a very weak band, which matches the calculated and scaled band at 2268 cm^{-1}.

Therefore, the matrix isolation experiments demonstrate that the photolysis of azide **1** yields triplet vinylnitrene ^{3}**2**, which is stable in the argon matrix, as it does not undergo intersystem crossing to form singlet products. However, vinylnitrene ^{3}**2** is photolabile, as it forms nitrile **3** upon prolonged irradiation.

Because the photolysis of azide **1** produces triplet vinylnitrene ^{3}**2**, which, upon further irradiation, yields nitrile **3**, we propose that the mechanism for forming vinylnitrene ^{3}**2** on the triplet surface of **1** is as shown in Scheme 3. Upon excitation, azide **1** forms its first singlet excited state (S_1), which intersystem crosses to its first triplet excited state (T_1). The

DOI: 10.1021/jacs.5b00998
J. Am. Chem. Soc. 2015, 137, 4207−4214

T_1 of **1** extrudes a N_2 molecule to yield triplet vinylnitrene ^{3}**2**, which is stable at 8 K (Scheme 3).

ESR Spectroscopy. A solution of azide **1** in MTHF was degassed by three freeze and thaw cycles at 2.5×10^{-2} Pa. The resulting solution was cooled to 5 K and irradiated for 10 s, and an ESR spectrum was recorded between 0 and 10 000 G. The spectrum showed X_2 and Y_2 lines typical of a nitrene at 6008 and 6224 G (Figure 3a). In addition, a broad signal at ∼4500 G

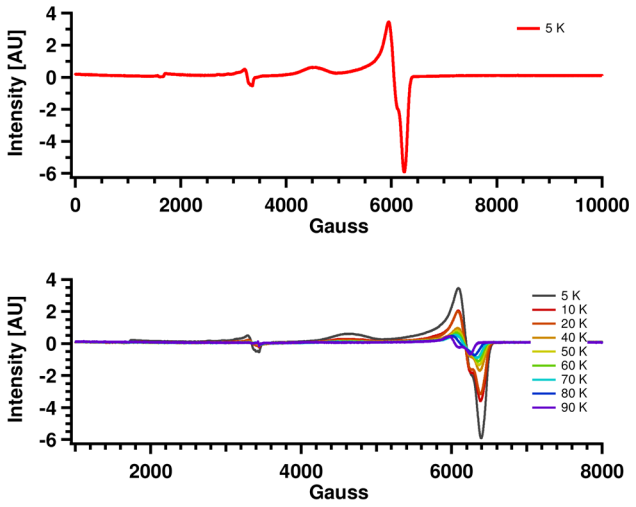

Figure 3. ESR spectra obtained by irradiating **1** in MTHF at (a) 5 K. (b) ESR signals as a function of temperature. Microwave frequency: 9.398 896 GHz; H_0 = 3353.5 G. X_2 = 6008 G; Y_2 = 6224 G; Z_1 ∼ 4500 G; Δm_s = 2−1685 G. D/hc = 0.7292 cm^{-1}. E/hc = 0.0048 cm^{-1}.

is found in the position expected for the Z_1 transition. The broadness of the signals is undoubtedly due to the use of an MTHF matrix. This makes the exact position of the Z_1 line uncertain, and it was not used in the calculation of the D and E values. A weak signal at ∼1685 G is also observed in Figure 3a, and this is most likely due to Δm_s = 2 (expected at 1676 cm^{-1}). The zero-field splitting parameters D/hc = 0.7292 cm^{-1} and E/hc = 0.0048 cm^{-1} were calculated on the basis of the X_2 and Y_2 lines using Wasserman's equations.[19] Warming of the matrix between 5 and 100 K caused the signal intensities to decrease, but the intensities were recovered upon recooling (Figure 3b). Thus, it can be concluded that vinylnitrene ^{3}**2** is stable up to at least 100 K.

The D and E values derived from Figure 3 are indicative of a delocalized nitrene. A linear correlation of D with the natural spin density on nitrogen ρ calculated at the UB3LYP/EPRIII level for over 100 nitrenes has been reported,[20] and the data for ^{3}**2** fit the graph precisely (see Supporting Information). However, the D and ρ values of naphthoquinon-2-ylnitrene ^{3}**2** (0.729 and 1.409) are significantly lower than those for 2-naphthylnitrene (0.925 and 1.521) but just slightly below those for 1-naphthylnitrene (0.793 and 1.449), which means that ^{3}**2** is more delocalized, i.e., more biradical-like, but it is definitely a nitrene. Other conjugated vinylnitrenes 4-cyanobutadienylnitrenes and 4-cyano-4-azabutadienylnitrenes have significantly lower D and ρ values 0.40−0.55 and 1.25−1.27, respectively.[16]

Transient Absorption Spectroscopy. The laser flash photolysis (excimer laser, 308 nm, 17 ns)[21] of **1** in argon-saturated acetonitrile produced a broad transient spectrum with λ_{max} ∼460 nm and a smaller shoulder at ∼350 nm (Figure 4). We assign this transient absorption to triplet vinylnitrene ^{3}**2** on

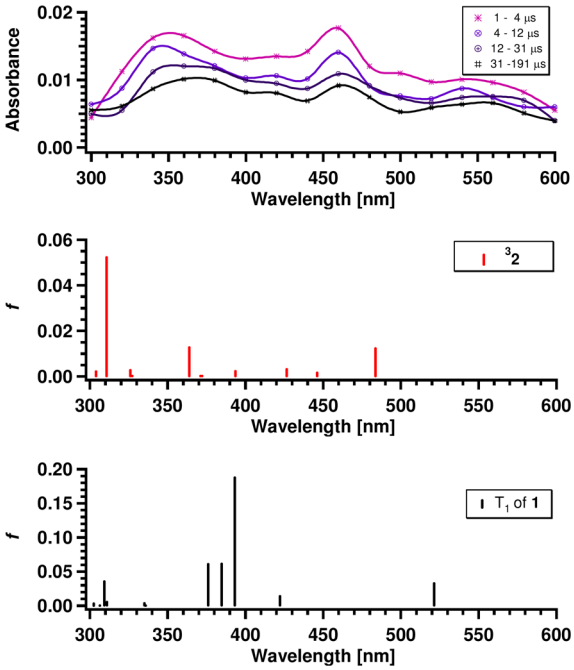

Figure 4. Transient UV−vis spectrum obtained by the laser flash photolysis of **1** in argon-saturated acetonitrile (top). Calculated electronic transitions (TD-DFT/B3LYP/6-31+G(d)) of triplet vinylnitrene ^{3}**2** (middle). Calculated electronic transitions (TD-DFT/B3LYP/6-31+G(d)) for T_1 of **1** (bottom).

the basis of the similarity between the observed transient spectrum and the time-dependent density functional theory (TD-DFT) calculated absorption spectrum of ^{3}**2**. The TD-DFT calculation places the major electronic transitions for ^{3}**2** at 311 nm (f = 0.0522), 364 nm (f = 0.0126), and 484 nm (f = 0.0122) (Figure 4), which fit nicely with the observed spectrum. In comparison, TD-DFT calculations predicted the most intense electronic transitions for the precursor T_1 of **1** (Figure 4) as being at 309 nm (f = 0.0352), 376 nm (f = 0.0605), 385 nm (f = 0.0611), 393 nm (f = 0.1872), and 521 nm (f = 0.0324), which does not fit the observed spectrum.

Kinetic analysis further supports the assignment of the transient absorption to triplet vinylnitrene ^{3}**2**, as the kinetic traces obtained at 350 and 460 nm in argon-saturated acetonitrile on shorter time scales can be fitted as monoexponential growth to yield a rate constant of 1.76×10^7 s^{-1} (τ ∼57 ns) for the formation of vinylnitrene ^{3}**2** from T_1 of **1**. At longer time scales, the decay of vinylnitrene ^{3}**2** yields a rate constant of 4.46×10^4 s^{-1} (τ ∼22 μs, Figure 5). A residual absorption that does not decay significantly on a millisecond time scale is ascribed to product formation.

In oxygen-saturated acetonitrile, the formation of vinylnitrene ^{3}**2** is faster than the time resolution of the laser flash apparatus (17 ns, Figure 5). Therefore, oxygen must reduce the lifetime of T_1 of **1**, leading to a much reduced yield of triplet vinylnitrene ^{3}**2**. No new absorption was detected that can be attributed to the addition of oxygen to vinylnitrene ^{3}**2** to form a peroxy radical, and it is concluded that the quenching of T_1 of **1** by oxygen is more efficient than the trapping of triplet vinylnitrene ^{3}**2**.

Low-Temperature UV−Vis Absorption Spectroscopy. Azide **1** was dissolved in MTHF with N_2 bubbled through the solution at room temperature for 10 min. The resulting solution was placed in liquid N_2, and its absorption spectrum

DOI: 10.1021/jacs.5b00998
J. Am. Chem. Soc. 2015, 137, 4207−4214

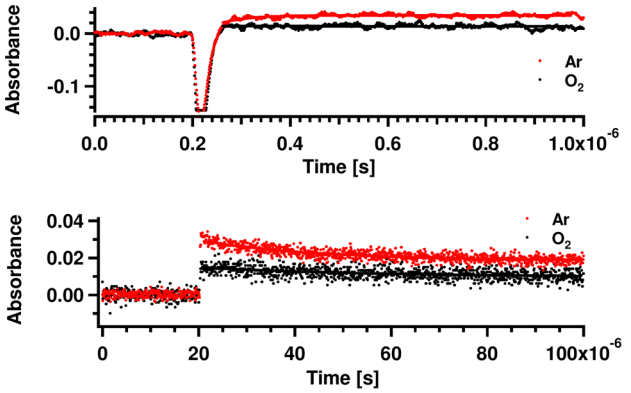

Figure 5. Kinetic traces obtained at 460 nm from the laser flash photolysis of **1** in argon-saturated (red) and oxygen-saturated (black) acetonitrile.

measured at 84 K showed a broad absorption between 320 and 410 nm with maximum absorption at approximately 350 and 390 nm due to the absorption of ground state of azide **1**, which is similar to the absorption spectrum of **1** at ambient temperature (Figure 6).

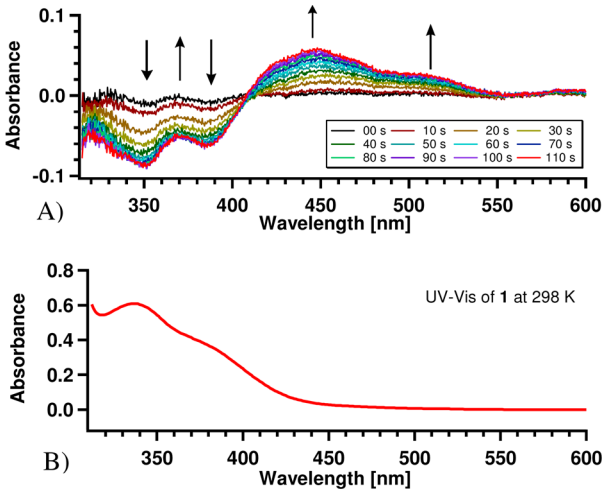

Figure 6. Absorption spectra obtained by irradiating **1** in (A) glassy MTHF matrix at 84 K and (B) MTHF solution at ambient temperature.

Irradiation of the glassy matrix with 340 nm light resulted in a broad new absorption band with λ_{max} at ~450 nm with small shoulders at approximately 370 and 520 nm (Figure 6). Further irradiation of the glassy MTHF matrix increased the intensity of these bands with simultaneous depletion of the absorptions at 350 and 390 nm ascribed to azide **1**. Because the absorption band at ~450 nm matches the transient absorption obtained by the laser flash photolysis of **1**, the absorption band at ~450 nm is assigned to triplet vinylnitrene ^{3}**2**. Thus, both the photolysis of azide **1** at ambient temperature and that in glassy matrices at 84 K resulted in the formation of triplet vinylnitrene ^{3}**2**.

Quantum Chemical Calculations. To better understand the reactivity of **1**, density functional theory (DFT) calculations were performed at the B3LYP/6-31+G(d) level of theory using Gaussian09.[22]

Time-dependent density functional theory (TD-DFT) calculations on the optimized structure of **1** places the first excited singlet state (S_1) of **1** at 63 kcal/mol above its S_0 and the first and second triplet excited states (T_1 and T_2) of **1** at 49 and 54 kcal/mol above the S_0 of **1**, respectively.

In comparison, the optimization of T_1 of **1** places it 46 kcal/mol above the S_0 of **1**. As expected, the calculated vertical energy of T_1 of **1** is only a few kcal/mol higher in energy than its relaxed structure. The optimized structure of T_1 of **1** has a (π,π*) configuration, as the $C_\alpha C_\beta$ bond has single bond character and the carbonyl groups have similar bond lengths as in the S_0 of **1** (Figure 7). Spin density calculations further

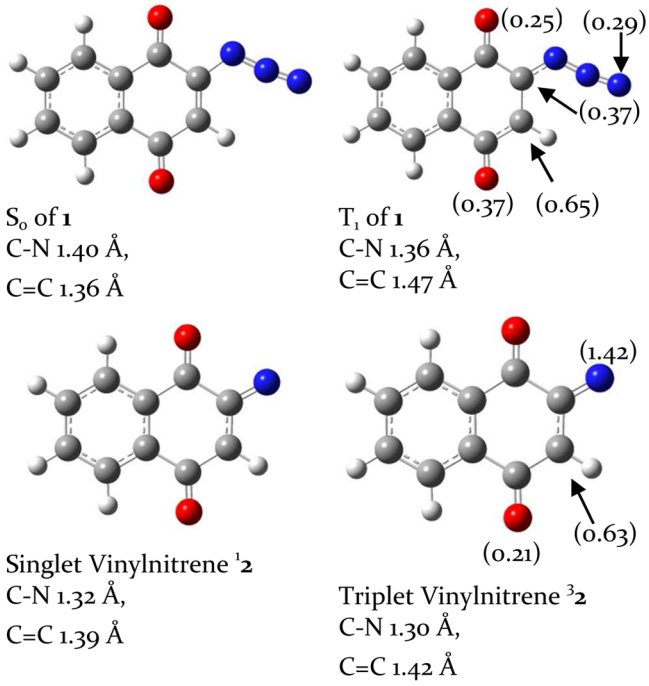

S_0 of **1**
C-N 1.40 Å,
C=C 1.36 Å

T_1 of **1**
C-N 1.36 Å,
C=C 1.47 Å

Singlet Vinylnitrene ^{1}**2**
C-N 1.32 Å,
C=C 1.39 Å

Triplet Vinylnitrene ^{3}**2**
C-N 1.30 Å,
C=C 1.42 Å

Figure 7. Optimized structures of **1**, T_1 of **1**, triplet vinylnitrene **2**, and singlet vinylnitrene ^{1}**2**. The calculated vinyl C═C and C—N bond lengths and spin densities (in parentheses) are listed.

support this assignment, as the unpaired spins are located on the α-C and β-C atoms and both the carbonyl oxygen atoms and the terminal N atom of the azido group, which are in conjugation with the α-C and β-C atoms.

The calculated spin density of vinylnitrene ^{3}**2** demonstrates that the unpaired spin is located mainly on the N atom (1.42) and the β-carbon atom (0.63). In addition, there is a small spin density on the carbonyl O atom (0.21), which is conjugated with the β-carbon atom (Figure 7). From these calculations, it can be concluded that vinylnitrene ^{3}**2** has significant 1,3-biradical character.

The calculated transition state for the formation of vinylnitrene ^{3}**2** from the T_1 of **1** was located only 2 kcal/mol above the triplet precursor and is therefore easily accessible. The stationary points on the triplet surface of **1** are plotted in Figure 8, which show that, upon the population of S_1 of **1**, it can undergo intersystem crossing to yield T_2 of **1**, which has an (n,π*) configuration, and then internal conversion to form T_1 of **1** with a (π,π*) configuration.

The open shell configuration of vinylnitrene ^{1}**2** was optimized using the broken-symmetry method with guess=mix as a keyword as featured in Gaussian09, resulting in a singlet nitrene with S2 value of 1.01. Optimization of the singlet vinylnitrene ^{1}**2** places it 16 kcal/mol higher in energy than triplet vinylnitrene ^{3}**2**. Therefore, the singlet–triplet energy gap

DOI: 10.1021/jacs.5b00998
J. Am. Chem. Soc. 2015, 137, 4207–4214

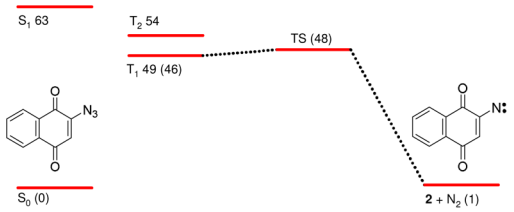

Figure 8. Calculated stationary points on the triplet surface of **1**. The energies of the S_1 (63), T_1 (49), and T_2 (54) of **1** were obtained from the TD-DFT calculations, whereas the energies of S_0 (0), T_1 (46), TS (48), and triplet vinyl nitrene ^{3}**2** were obtained by optimization calculations. Energies are in kcal/mol.

for **2** is similar to the values calculated for several other vinylnitrene derivatives.[7−9,17]

Although triplet vinylnitrene ^{3}**2** did not produce azirine **4** or ketenimine **5** in cryogenic matrices, we optimized the structures of these compounds to determine whether their formation is energetically feasible (Scheme 4). Ketenimine **5** is 16 kcal/mol

Scheme 4. Potential Product of the Intersystem Crossing of Triplet Vinylnitrene ^{3}2

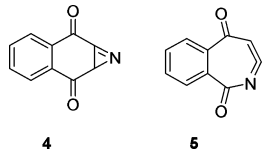

more stable than vinylnitrene ^{3}**2**, whereas azirine **4** is isoenergetic with vinylnitrene ^{3}**2**. Thus, azirine **4** must possess considerable ring strain and is expected to be highly reactive.

We calculated the stationary points on the triplet surface of vinylnitrene ^{3}**2** for the formation of nitrile **3** (Figure 9). The

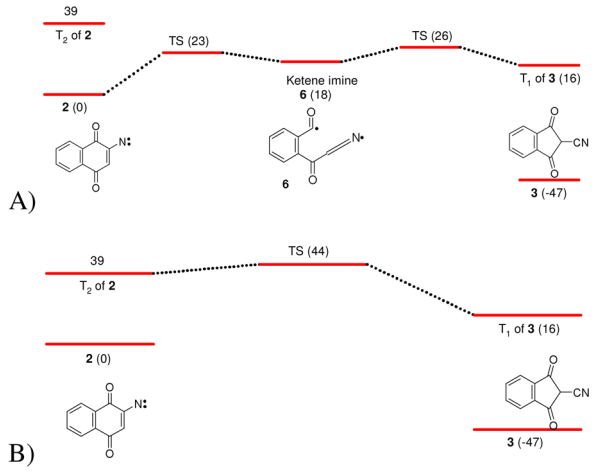

Figure 9. Calculated energy surfaces for triplet vinylnitrene ^{3}**2** forming nitrile **3** on the triplet surface: (A) stepwise and (B) concerted. Energies are in kcal/mol.

transition state for vinylnitrene ^{3}**2** forming the T_1 of nitrile **3** was located 44 kcal/mol above vinylnitrene ^{3}**2** (Figure 9B). Thus, the formation of nitrile **3** is accessible upon the excitation of vinylnitrene ^{3}**2**.

The formation of nitrile **3** can also take place by the photoinduced α-cleavage of vinylnitrene ^{3}**2** to form a ketenimine radical **6**, which rearranges into nitrile **3** (Figure 9A). The calculated transition state for the α-cleavage of vinylnitrene ^{3}**2** to form this ketenimine radical is 23 kcal/mol and is therefore easily accessible photochemically. The transition state for the rearrangement of ketenimine radical **6** to form T_1 of **3** is only 8 kcal/mol above **6** and is thus also very feasible. Because the formation of nitrile **3** requires intersystem crossing to the singlet surface, it is reasonable that ketenimine radical **6** intersystem crosses to form the S_0 of nitrile **3** rather than T_1 of **3**. Thus, the calculations support the observation that vinylnitrene ^{3}**2** forms nitrile **3** photochemically, and the formation of this nitrile in a stepwise reaction seems more favorable.

Product Analysis. Naruta et al. have shown previously that the photolysis of azide **1** in the presence of 2,4-hexadiene yields cycloaddition products **7** and **8** (Scheme 5).[23] We repeated this

Scheme 5. Trapping of Triplet Vinylnitrene ^{3}2 with 2,4-Hexadiene

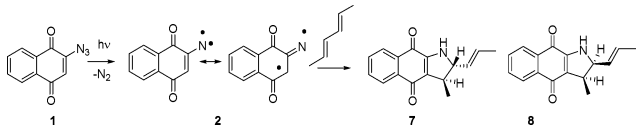

experiment and obtained the same results. Adducts **7** and **8** must be formed by trapping triplet vinylnitrene ^{3}**2** with the diene. In comparison, the photolysis of azide **1** in chloroform, methanol, and acetonitrile at room temperature results in a polymeric tar. The product studies indicate that vinylnitrene ^{3}**2** is sufficiently long-lived to be intercepted in bimolecular reactions, whereas, in the absence of a trapping agent, it forms products that are not stable enough to be isolated.

DISCUSSION

Intramolecular sensitization makes it possible to form triplet vinylnitrene ^{3}**2** efficiently from azide **1**. The T_1 of **1** has a (π,π^*) configuration, which resembles a triplet 1,2-biradical that is stabilized by the adjacent carbonyl and azido groups. T_1 of **1** is an excellent precursor to triplet vinylnitrene ^{3}**2**, as the biradical centers are lined up perfectly to reform the vinylic C═C bond upon extrusion of the N_2 molecule (Scheme 6). In

Scheme 6. Formation of Triplet Vinylnitrenes from the (π,π^*) Triplet Excited State of 1 and 1,2-Biradical Forms of Triplet Excited Vinyl Azides

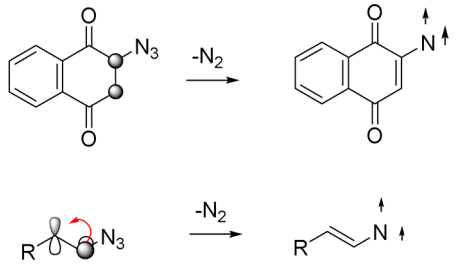

comparison, the formation of vinylnitrenes by the intramolecular sensitization of simple azidoalkenes yield orthogonal 1,2-biradicals to minimize the repulsion between the two radical centers; therefore, these two radical centers have to rotate to reform the vinylic C═C bond and extrude the N_2 molecule.[17]

Because triplet vinylnitrene ^{3}**2** is stable at cryogenic temperatures, it was observed directly by IR and ESR

DOI: 10.1021/jacs.5b00998
J. Am. Chem. Soc. 2015, 137, 4207−4214

spectroscopy, although further irradiation causes ^{3}**2** to rearrange to nitrile **3**. Wenthold and Hossain have demonstrated that radical stabilization by electron delocalization effectively reduces the triplet−singlet energy gap of vinylnitrenes.[24] However, the calculated energy gap between the open shell singlet and triplet configuration of vinylnitrene **2** of 16 kcal/mol is similar to the calculated energy gap for vinylnitrenes **9**, **10**, and **11**, which are not stable in cryogenic argon matrices (Scheme 7), as they form ketenimines.[7−9] Therefore, the stability of vinylnitrene ^{3}**2** cannot be credited to an unusually large energy gap between its singlet and triplet configurations.

Scheme 7. Calculated Rotation Barrier around the C—C═C—N Bond in Triplet Vinylnitrenes 9, 10, and 11 and Spin Densities on N and C Atoms

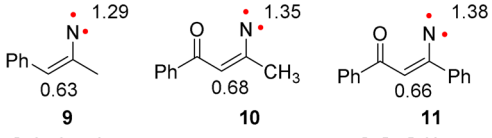

9 **10** **11**

Calculated rotational barrier around the C-C=C-N bond

10 11 7.5 kcal/mol

The properties of triplet vinylnitrene ^{3}**2** are reminiscent of triplet phenyl- and alkylnitrenes, which are also stable in cryogenic matrices and have been identified directly using ESR, UV−vis, and IR spectroscopy.[14,25−28] The significant difference between triplet vinylnitrenes and alkyl- and phenylnitrenes is that the latter ones do not react via intersystem crossing to the singlet states but rather by dimerization. Because the singlet−triplet energy gap for alkylnitrenes is large (31.2 kcal/mol for methylnitrene),[29] they are not expected to undergo intersystem cross efficiently, as intersystem crossing is enhanced by small energy gaps and spin−orbit coupling. In comparison, the singlet−triplet energy gap for phenylnitrene has been measured as 15 kcal/mol,[30] which is similar to the calculated energy gap for vinylnitrenes **2**, **9**, **10**, and **11**, which raises the question of why these nitrenes react so differently. A comparison of the calculated spin density for triplet phenylnitrene and vinylnitrene **2** demonstrates that the spin density in vinylnitrene ^{3}**2** is localized to a greater extent on the β-C atom than in the case for phenylnitrene. We have previously reported the calculated spin densities of vinylnitrenes **9**, **10**, and **11**, which are similar to those of vinylnitrene ^{3}**2**. Thus, the most significant difference between triplet vinylnitrenes **2**, **9**, **10**, and **11** on one hand and triplet phenylnitrene on the other is that the vinylnitrenes have more 1,3-biradical character, which makes rotation around the vinylic C═C bond feasible for vinylnitrenes **9**, **10**, and **11**. The ring structure of vinylnitrene ^{3}**2**, however, severely limits the rotation around its vinylic bond. The calculated rotational barriers around the vinylic C═C bond for triplet vinylnitrenes **9**, **10**, and **11** are only between 7.5 and 11 kcal/mol due to their significant 1,3-biradical characters (Scheme 7). Thus, we propose that a major reason for the stability of vinylnitrene ^{3}**2** in matrices is due to its rigid cyclic structure, which limits rotation around the vinylic C═C bond. For triplet biradicals to intersystem cross and form ground-state products, they need to acquire the conformation best suited for intersystem crossing, concurrently with new bond formation.[31] Because the triplet vinylnitrenes **9**, **10**, and **11** can rotate around their vinylic C═C bond, they are flexible and should undergo intersystem crossing to form products more efficiently than vinylnitrene ^{3}**2**. Conversely, triplet phenylnitrene derivatives do not decay by intersystem crossing, as the phenyl ring also prohibits rotation around the aromatic bonds. The calculated spin density of vinylnitrene ^{3}**2** explains nicely why it reacts efficiently with alkenes to form adducts **7** and **8** (Scheme 5). Similarly, the spin density of phenylnitrene also reflects that it undergoes dimerization to form azobenzene (Scheme 8).

Scheme 8. Comparison of the Calculated Spin Densities for Triplet Vinylnitrene ^{3}2 and Phenylnitrene

CONCLUSION

We have shown that triplet vinylnitrene ^{3}**2** is formed efficiently through intramolecular triplet sensitization upon irradiation of vinyl azide **1**. Triplet vinylnitrene ^{3}**2** was thermally stable in cryogenic matrices up to at least ∼100 K and was characterized directly by ESR and IR spectroscopy. Under the irradiation conditions in the Ar-matrix at 8 K, a novel photoinduced rearrangement reaction of vinylnitrene ^{3}**2** was found to give nitrile **3**. The ESR spectroscopy demonstrates that triplet vinylnitrene ^{3}**2** has a significant 1,3-biradical character, as previously perceived from calculations. Because triplet vinylnitrene ^{3}**2** is part of a bicyclic ring system, it is rigid, which restricts the rotation around the vinylic C═C bond and renders it more stable than other vinylnitrenes due to less facile intersystem crossing. Thus, we have demonstrated that the unique reactivity of triplet vinylnitrenes is due to their flexibility, which is a reflection of their significant 1,3-biradical character. Triplet vinylnitrenes can be stabilized by limiting the flexibility of the vinyl C═C bond; thus, it may be possible to design various triplet vinylnitrenes as potential building blocks for high-spin assemblies.

EXPERIMENTAL SECTION

Matrix IR Spectroscopy. First, argon was deposited at 20 K for 5 min on a CsI target inside the cryostat cold head. The sample was then sublimed at 50 °C and deposited with argon at 20 K for 10 min in the vacuum of a diffusion pump. The cryostat cold head was cooled to 8 K for sample irradiation. The argon matrix containing the deposited molecules of **1** was irradiated through quartz windows using a 320−360 nm filter, and IR spectra were collected after various irradiation times.

ESR Spectroscopy. A 0.15 mM solution of **1** in anhydrous MTHF was degassed by three freeze/thaw cycles using diffusion and rotary pumps. The tube containing the solution was sealed after degassing and used for ESR spectroscopy measurements. ESR spectra were recorded on a Bruker instrument.

Quantum Chemical Calculations. The ground states, triplet excited states, vinyl nitrene (**2**), and product (**3**) were optimized by performing density functional theory (DFT) calculations using Gaussian09 at the B3LYP level of theory with the 6-31+G(d) basis set.[22,32,33] The natural spin densities were calculated at the UB3LYP/EPRIII level as implemented in Gaussian03.[34] To obtain the calculated UV−vis spectra for the excited states and intermediates, time-dependent DFT (TD-DFT) calculations were conducted at the B3LYP level of theory with the 6-31+G(d) basis set. The same type of calculation was used to locate the excited singlet (S_1) and triplet states (T_1, T_2) of the azide **1**. The transition states were confirmed to contain one imaginary vibrational frequency by the analytical

DOI: 10.1021/jacs.5b00998
J. Am. Chem. Soc. 2015, 137, 4207−4214

determination of the second derivative of the energy with respect to the internal coordinates. Intrinsic reaction coordinate (IRC) calculations were used to verify that the transition state is correlated with the vinyl nitrene (**2**) and the triplet excited state of starting material **1**.[35,36]

Laser Flash Photolysis. An excimer laser (308 nm, 17 ns) was used for laser flash photolysis (LFP) in solution.[21] A stock solution of **1** was made up in acetonitrile with spectroscopic grade solvent such that the absorbance of the solutions was 0.3−0.8 at 308 nm. Quartz cuvettes with 10 mm × 10 mm cross section were used. Before each measurement, approximately 2 mL of the stock solution was added to the cuvette, which was then purged with argon for approximately 5 min. The growth and decay traces were fitted using Igor Pro software.

Preparation of 1. In a 100 mL round-bottomed flask, 2-bromo-1,4-naphthoquinone (1.000 g, 4.219 mmol) was dissolved in acetone (40 mL), and then sodium azide (0.329 g, 5.063 mmol) was added to the solution in portions. The reaction mixture was stirred for 24 h, acetone was removed under reduced pressure, and the residue was dissolved in diethyl ether. The ether solution was washed several times with water and dried over magnesium sulfate, and the solvent was removed under reduced pressure to yield pure **1** (0.722 g, 3.628 mmol, 86% yield). The IR and ^{1}H NMR spectra of **1** were in accordance with the literature data.[37] ^{1}H NMR (400 MHz, $CDCl_3$): δ 8.14−8.09 (m, 2H), 7.79−7.75 (m, 2H), 6.47 (s, 1H) ppm. IR (neat): 2920, 2122, 2103, 1676, 1650, 1596, 1574, 1371, 1271, 1123 cm^{-1}.

Preparative Photolysis of 1. Azide **1** (10 mg, 0.050 mmol) and 2,4-hexadiene (82 mg, 1.0 mmol) were dissolved in benzene (8 mL), and N_2 was bubbled through the solution for 10 min. The resulting solution was irradiated using a mercury lamp and an aqueous solution of $CuSO_4$ (>334 nm, 250 g/L) as a filter at 20 °C for 75 min. The GC-MS analysis of the reaction mixture showed the formation of two new products in a ratio of 3:2, and almost all the starting material had been consumed. The photoproducts both had a mass of 253 g/mol, in agreement with a report by Naruta et al.[23]

■ ASSOCIATED CONTENT

Supporting Information

^{1}H NMR and IR spectra of **1**; graph showing the correlation of D with the natural spin densities ρ for several nitrenes; Cartesian coordinates and energies of **1**−**5**; difference IR spectra in Ar matrices. This material is available free of charge via the Internet at http://pubs.acs.org.

■ AUTHOR INFORMATION

Corresponding Author

anna.gudmundsdottir@uc.edu

Notes

The authors declare no competing financial interest.

■ ACKNOWLEDGMENTS

We thank the National Science Foundation and the Ohio Supercomputer Center for their generous support of this work. A.D.G. is grateful to the Fulbright Foundation for giving her the opportunity to be a Fulbright Scholar in Professor Abe's laboratory at Hiroshima University. This work was supported by a Grant-in-Aid for Science Research on Innovative Areas "Stimuli-responsive Chemical Species" (No. 24109008) from the Ministry of Education, Culture, Sports, Science and Technology, Japan. ESR and MS measurements were performed at N-BARD, Hiroshima University.

■ REFERENCES

(1) *Nitrenes and Nitrenium Ions*; Falvey, D. E., Gudmundsdottir, A. D., Eds.; Wiley Series on Reactive Intermediates in Chemistry and Biology; John Wiley & Sons, Inc.: New York, 2013; Vol. 6.
(2) Platz, M. S. In *Reactive Intermediate Chemistry*; Moss, R. A., Platz, M. S., Jones, M., Jr., Eds.; John Wiley & Sons, Inc.: New York, 2004.
(3) Jadhav, A. V.; Gulgas, C. G.; Gudmundsdottir, A. D. *Eur. Polym. J.* **2007**, *43*, 2594−2603.
(4) Sterner, O.; Serrano, Â.; Mieszkin, S.; Zürcher, S.; Tosatti, S.; Callow, M. E.; Callow, J. A.; Spencer, N. D. *Langmuir* **2013**, *29*, 13031−13041.
(5) Platz, M. S. *Photochem. Photobiol.* **1997**, *65*, 193−194.
(6) Tomioka, H. In *Reactive Intermediate Chemistry*; Platz, M. S., Moss, R. A., Jones, J. M., Eds.; John Wiley: Hoboken, NJ, 2004; p 375.
(7) Gamage, D. W.; Li, Q.; Ranaweera, R. a. a. U.; Sarkar, S. K.; Weragoda, G. K.; Carr, P. L.; Gudmundsdottir, A. D. *J. Org. Chem.* **2013**, *78*, 11349−11356.
(8) Zhang, X.; Sarkar, S. K.; Weragoda, G. K.; Rajam, S.; Ault, B. S.; Gudmundsdottir, A. D. *J. Org. Chem.* **2014**, *79*, 653−663.
(9) Rajam, S.; Murthy, R. S.; Jadhav, A. V.; Li, Q.; Keller, C.; Carra, C.; Pace, T. C. S.; Bohne, C.; Ault, B. S.; Gudmundsdottir, A. D. *J. Org. Chem.* **2011**, *76*, 9934−9945.
(10) Nunes, C. M.; Reva, I.; Pinho e Melo, T. M. V. D.; Fausto, R.; Šolomek, T.; Bally, T. *J. Am. Chem. Soc.* **2011**, *133*, 18911−18923.
(11) Nunes, C. M.; Reva, I.; Fausto, R. *J. Org. Chem.* **2013**, *78*, 10657−10665.
(12) Inui, H.; Murata, S. *Chem. Commun.* **2001**, 1036−1037.
(13) Inui, H.; Murata, S. *Chem. Lett.* **2001**, *30*, 832−833.
(14) Singh, P. N. D.; Mandel, S. M.; Sankaranarayanan, J.; Muthukrishnan, S.; Chang, M.; Robinson, R. M.; Lahti, P. M.; Ault, B. S.; Gudmundsdóttir, A. D. *J. Am. Chem. Soc.* **2007**, *129*, 16263−16272.
(15) Schrock, A. K.; Schuster, G. B. *J. Am. Chem. Soc.* **1984**, *106*, 5228−5234.
(16) Wentrup, C.; Kvaskoff, D. *Aust. J. Chem.* **2013**, *66*, 286−296.
(17) Rajam, S.; Jadhav, A. V.; Li, Q.; Sarkar, S. K.; Singh, P. N. D.; Rohr, A.; Pace, T. C. S.; Li, R.; Krause, J. A.; Bohne, C.; Ault, B. S.; Gudmundsdottir, A. D. *J. Org. Chem.* **2014**, *79*, 9325−9334.
(18) Foresman, J. B.; Frisch, Æ. *Exploring Chemistry with Electronic Structure Methods*; Gaussian, Inc.: Pittsburgh, PA, 1996.
(19) Wasserman, E.; Snyder, L. C.; Yager, W. A. *J. Chem. Phys.* **1964**, *41*, 1763−1772.
(20) Kvaskoff, D.; Bednarek, P.; George, L.; Waich, K.; Wentrup, C. *J. Org. Chem.* **2006**, *71*, 4049−4058.
(21) Muthukrishnan, S.; Sankaranarayanan, J.; Klima, R. F.; Pace, T. C. S.; Bohne, C.; Gudmundsdottir, A. D. *Org. Lett.* **2009**, *11*, 2345−2348.
(22) Frisch, M. J.; Trucks, G. W.; Schlegel, H. B.; Scuseria, G. E.; Robb, M. A.; Cheeseman, J. R.; Scalmani, G.; Barone, V.; Mennucci, B.; Petersson, G. A.; Nakatsuji, H.; Caricato, M.; Li, X.; Hratchian, H. P.; Izmaylov, A. F.; Bloino, J.; Zheng, G.; Sonnenberg, J. L.; Hada, M.; Ehara, M.; Toyota, K.; Fukuda, R.; Hasegawa, J.; Ishida, M.; Nakajima, T.; Honda, Y.; Kitao, O.; Nakai, H.; Vreven, T.; Montgomery, J. A., Jr.; Peralta, J. E.; Ogliaro, F.; Bearpark, M.; Heyd, J. J.; Brothers, E.; Kudin, K. N.; Staroverov, V. N.; Kobayashi, R.; Normand, J.; Raghavachari, K.; Rendell, A.; Burant, J. C.; Iyengar, S. S.; Tomasi, J.; Cossi, M.; Rega, N.; Millam, J. M.; Klene, M.; Knox, J. E.; Cross, J. B.; Bakken, V.; Adamo, C.; Jaramillo, J.; Gomperts, R.; Stratmann, R. E.; Yazyev, O.; Austin, A. J.; Cammi, R.; Pomelli, C.; Ochterski, J. W.; Martin, R. L.; Morokuma, K.; Zakrzewski, V. G.; Voth, G. A.; Salvador, P.; Dannenberg, J. J.; Dapprich, S.; Daniels, A. D.; Farkas, O.; Foresman, J. B.; Ortiz, J. V.; Cioslowski, J.; Fox, D. J. *Gaussian 09*, revision a.02; Gaussian, Inc.: Wallingford, CT, 2009.
(23) Naruta, Y.; Yokota, T.; Nagai, N.; Maruyama, K. *J. Chem. Soc., Chem. Commun.* **1986**, 972−973.
(24) Wenthold, P. G. *J. Org. Chem.* **2011**, *77*, 208−214.
(25) Kuck, V. J.; Wasserman, E.; Yager, W. A. *J. Phys. Chem.* **1972**, *76*, 3570−3571.
(26) Wasserman, E.; Smolinsky, G.; Yager, W. A. *J. Am. Chem. Soc.* **1964**, *86*, 3166−3167.
(27) Hayes, J. C.; Sheridan, R. S. *J. Am. Chem. Soc.* **1990**, *112*, 5879−5881.

DOI: 10.1021/jacs.5b00998
J. Am. Chem. Soc. 2015, 137, 4207−4214

(28) Reiser, A.; Terry, G. C.; Willets, F. W. *Nature* **1966**, *211*, 410−410.
(29) Travers, M. J.; Cowles, D. C.; Clifford, E. P.; Ellison, G. B.; Engelking, P. C. *J. Chem. Phys.* **1999**, *111*, 5349.
(30) Wijeratne, N. R.; Da Fonte, M.; Ronemus, A.; Wyss, P. J.; Tahmassebi, D.; Wenthold, P. G. *J. Phys. Chem. A* **2009**, *113*, 9467−9473.
(31) Michl, J. *J. Am. Chem. Soc.* **1996**, *118*, 3568−3579.
(32) Becke, A. D. *J. Chem. Phys.* **1993**, *98*, 5648−5652.
(33) Lee, C.; Yang, W.; Parr, R. G. *Phys. Rev. B* **1988**, *37*, 785−789.
(34) Frisch, M. J.; Trucks, G. W.; Schlegel, H. B.; Scuseria, G. E.; Robb, M. A.; Cheeseman, J. R.; Montgomery, J. A., Jr.; Vreven, T.; Kudin, K. N.; Burant, J. C.; Millam, J. M.; Iyengar, S. S.; Tomasi, J.; Barone, V.; Mennucci, B.; Cossi, M.; Scalmani, G.; Rega, N.; Petersson, G. A.; Nakatsuji, H.; Hada, M.; Ehara, M.; Toyota, K.; Fukuda, R.; Hasegawa, J.; Ishida, M.; Nakajima, T.; Honda, Y.; Kitao, O.; Nakai, H.; Klene, M.; Li, X.; Knox, J. E.; Hratchian, H. P.; Cross, J. B.; Bakken, V.; Adamo, C.; Jaramillo, J.; Gomperts, R.; Stratmann, R. E.; Yazyev, O.; Austin, A. J.; Cammi, R.; Pomelli, C.; Ochterski, J. W.; Ayala, P. Y.; Morokuma, K.; Voth, G. A.; Salvador, P.; Dannenberg, J. J.; Zakrzewski, V. G.; Dapprich, S.; Daniels, A. D.; Strain, M. C.; Farkas, O.; Malick, D. K.; Rabuck, A. D.; Raghavachari, K.; Foresman, J. B.; Ortiz, J. V.; Cui, Q.; Baboul, A. G.; Clifford, S.; Cioslowski, J.; Stefanov, B. B.; Liu, G.; Liashenko, A.; Piskorz, P.; Komaromi, I.; Martin, R. L.; Fox, D. J.; Keith, T.; Al-Laham, M. A.; Peng, C. Y.; Nanayakkara, A.; Challacombe, M.; Gill, P. M. W.; Johnson, B.; Chen, W.; Wong, M. W.; Gonzalez, C.; Pople, J. A. *Gaussian 03*, revision c.02; Gaussian, Inc.: Wallingford, CT, 2003..
(35) Gonzalez, C.; Schlegel, H. B. *J. Chem. Phys.* **1989**, *90*, 2154−2161.
(36) Gonzalez, C.; Schlegel, H. B. *J. Phys. Chem.* **190**, *94*, 5523−5527.
(37) Couladouros, E. A.; Plyta, Z. F.; Haroutounian, S. A.; Papageorgiou, V. P. *J. Org. Chem.* **1997**, *62*, 6−10.

DOI: 10.1021/jacs.5b00998
J. Am. Chem. Soc. 2015, 137, 4207−4214